

Fermi National Accelerator Laboratory

FERMILAB-Conf-90/125-E  
[E-665]

**Preliminary Results from E665 on Cross-Section Ratios at  
Low  $x_{bj}$  Using  $H_2$ ,  $D_2$  and Xe Targets \***

The E665 Collaboration

*presented by*

Silhacén Aïd  
*University of Maryland  
College Park, Maryland 20742*

June 1990

\* Presented at the Workshop on Hadron Structure Functions and Parton Distributions, Batavia, Illinois, April 26-28, 1990.



**Preliminary Results from E665 on Cross-Section Ratios  
at Low  $x_b$ , Using H<sub>2</sub>, D<sub>2</sub> and Xe Targets**

*Silhacén Aïd*

*Department of Physics and Astronomy, University of Maryland  
College Park MD 20742, USA*

*for the E665 collaboration*

**Abstract**

Fermilab experiment 665 has taken deep-inelastic muon scattering data at a beam energy of 490 GeV/c, on H<sub>2</sub>, D<sub>2</sub> and Xe targets. Two triggers have been used : a large scattering-angle trigger (LAT), sensitive to a minimum scattering angle of 3 mrad, and a small scattering-angle trigger which can accept a scattering angle down to 0.5 mrad. The neutron to proton ratio is reported for  $x_b$  above 0.002, and it shows consistency with 1 as  $x_b$  goes to 0. The Xe to D<sub>2</sub> cross-section ratio is reported for  $x_b$  above 0.001 and it shows evidence of shadowing.

## 1. The E665 experiment

The purpose of E665 is to study the scattering process  $\mu + N \rightarrow \mu + X$ , where  $N$  represents a nucleon and  $X$  a hadronic final state (Fig.1).

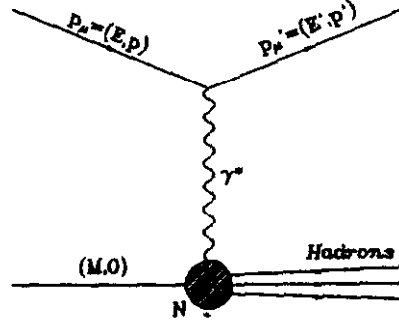


Fig.1

If  $p_\mu = (E, \vec{p})$  and  $p'_\mu = (E', \vec{p}')$  represent the 4-momenta of the incident and scattered muon respectively, and  $M$  the mass of the target nucleon, the relevant kinematic variables are

$$\begin{aligned} Q^2 &= -(p_\mu - p'_\mu)^2 \\ \nu &= E - E' \\ y &= \frac{\nu}{E} \\ x_{bj} &= \frac{Q^2}{2M\nu} \end{aligned}$$

and the cross-section for this process, in the one-photon exchange approximation is given by

$$\frac{d\sigma}{dQ^2 dx} = \frac{4\pi\alpha^2}{Q^4 x} (y^2 x F_1(x, Q^2) + (1 - y - Mxy/2E) F_2(x, Q^2))$$

The spectrometer used for this purpose has been described elsewhere<sup>1</sup>, but for the sake of completeness, we shall give a brief overview of its main features. A view of the apparatus is shown in Fig.2.

### 1.1 Beam

800 GeV/c protons from the Fermilab Tevatron interact with a beryllium target to produce pions and kaons which decay into muons, the average momentum of which is 490 GeV/c, with a spread of about 60 GeV/c. The beam tracks are

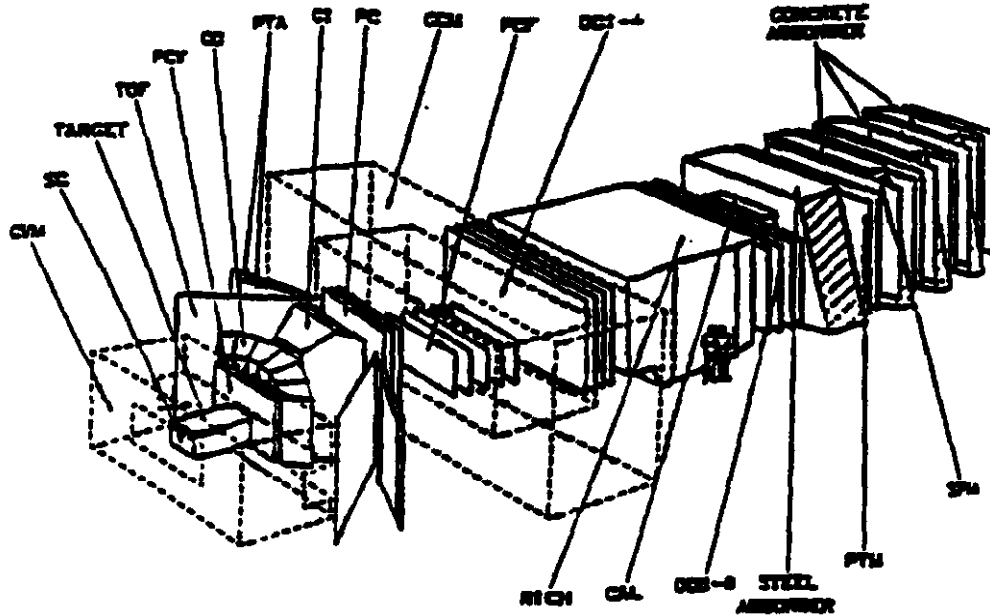


Fig. 2  
View of the E665 spectrometer

reconstructed using a set of 24 wire-chamber planes, and the bending induced by an analyzing magnet is measured and the momentum determined, with a resolution of 0.5% at 500 GeV/c.

### 1.2 Forward spectrometer

The muon beam interacts with a target located inside a superconducting magnet (CVM). The charged hadrons and the scattered muon resulting from the interaction are detected by sets of proportional wire chambers and drift chambers. The momentum measurement is done by an other superconducting magnet (CCM) located downstream from the target, with a resolution of 2.5% at 500 GeV. Neutral particles are detected by an electromagnetic calorimeter.

### 1.3 Triggering system

Events are triggered by detection of the scattered muon in a set of four scintillator stations located behind a 3-metre thick hadron absorber. Two triggers have been used to get the data presented here. A large-angle trigger (LAT) requires

a signal in at least 3 out of 4 scintillator walls and the absence of a signal in a fixed veto region centered around the beam. This trigger has reasonable acceptance for scattering angles above 3 mrad.

The small-angle trigger (SAT) is a floating-veto trigger. A fraction of the beam is projected to the absorber and the predicted impact point is compared with the actual muon position. If the latter falls outside a window centered around the beam projection the event is accepted. The minimum scattering angle to which this trigger has good acceptance is 0.5 mrad.

## 2. The neutron-to-proton ratio

### 2.1 Physics motivation

At low  $x_{bj}$ , the contribution to the deep-inelastic cross-section originates predominantly from the sea. The valence-quark contribution becomes negligible, and insofar as the sea distributions are the same in neutrons and protons, the ratio  $\sigma_n/\sigma_p$ , defined as

$$\sigma_n/\sigma_p = \frac{\sigma_D - \sigma_H}{\sigma_H}$$

(where  $\sigma_p$  is the proton cross-section,  $\sigma_n$  is the neutron cross-section,  $\sigma_D$  is the nuclear deuterium cross-section and  $\sigma_H$  the hydrogen cross-section, integrated over a given  $x_{bj}$  bin), should go to 1 as  $x_{bj}$  goes to 0. Previous measurements<sup>2,3</sup> suggest that this is indeed the case. The E665 contribution is at lower values of  $x_{bj}$  which have not been reached before.

### 2.2 Preliminary results

The measurement of the neutron-to-proton ratio has been performed at low  $x_{bj}$  using the large-angle trigger (LAT) and the small-angle trigger (SAT). The average  $Q^2$  for the LAT is 15 GeV<sup>2</sup>, with a minimum of 4 GeV<sup>2</sup>, that of the SAT is 3.6 GeV<sup>2</sup>, with a minimum  $Q^2$  of 0.1 GeV<sup>2</sup>. For the LAT data, a minimum  $x_{bj}$  cut of 0.005 was made, and a minimum  $x_{bj}$  of 0.002 was imposed on the SAT data. The results are shown in Fig.3. It can be seen that as  $x_{bj}$  approaches 0, the ratio is consistent with 1 within errors.

### 2.3 Estimate of systematic errors

Even though most systematic effects cancel out in the measurement of cross-section ratios, the fact that data for different targets were taken at different time periods introduces systematic effects due to variations in the running conditions. The sources of systematic uncertainties are :

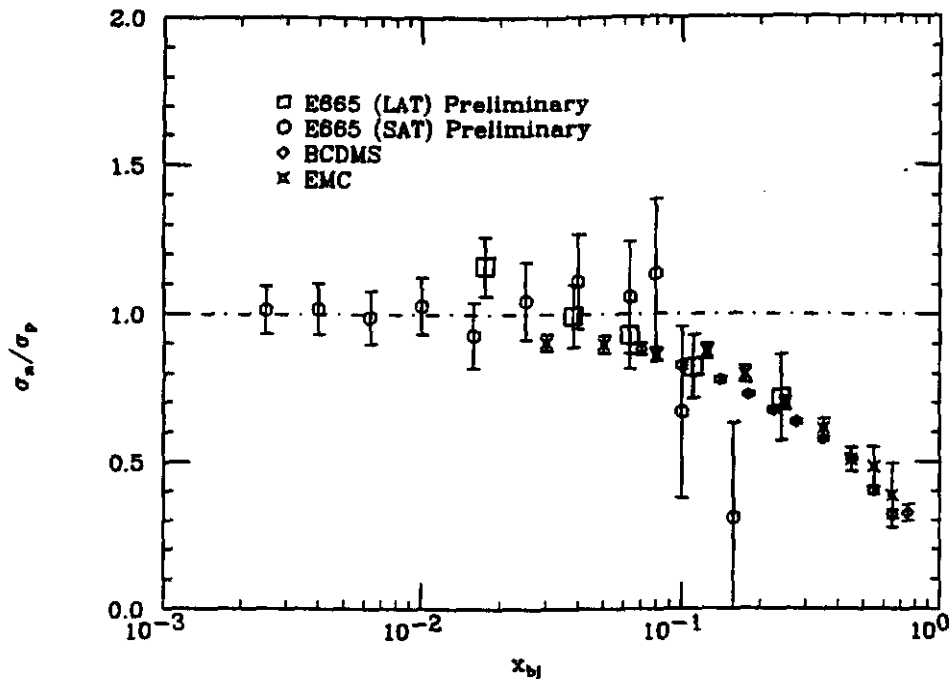


**Fig. 3**  
Neutron-to-proton ratio as a function of  $x_{bj}$

BCDMS points are from reference 3. EMC points from reference 2.

- *Beam normalization* : The correctness of the number of live beams was done by comparing "event" scalers, which count the number of beams during the live time of the experiment, against randomly preselected beams. When the prescale factor is taken into account, both numbers agree to better than 1/2%. In addition, the random beams allowed to factor out the beam-reconstruction efficiency. We currently estimate the normalization uncertainty to be around 1%.
- *Reconstruction efficiency* , due to variation in time of detector performance; this is currently under investigation, and we attribute to this correction a value not to exceed 10%.
- *Empty-target subtraction* : correction of the order of 1 to 2%.
- *Target density* : uncertainty estimated to be 1%.
- *Radiative correction* : the correction on the  $n/p$  ratio is less than 1%.
- *Fermi motion* : negligible at low  $x_{bj}$ <sup>3</sup>.

### 3. Xe to D<sub>2</sub> cross-section ratio

#### 3.1 Physics motivation

Compared to the parton distributions of single nucleons, those of nuclei are modified by the nuclear environment. Previous measurements<sup>4</sup> have shown that at low  $x_{b,j}$ , the deep-inelastic cross-section (per nucleon) on nuclear targets is smaller than that of single nucleons, a phenomenon known as shadowing. E665 has compared the xenon cross-section to the deuterium cross-section and observed a similar effect.

#### 3.2 Preliminary results

At low  $x_{b,j}$ , radiative processes are an important background to deep inelastic scattering in Xe. The traditional approach used by previous experiments was on the one hand to restrict the kinematic range of the data by essentially imposing an upper cut on the energy transfer  $\nu$ , and on the other hand to apply corrections based on numerical calculations of the radiative contribution to deep inelastic scattering, using Mo and Tsai formalism or more accurate formulae such as those of Bardin et al., in which higher-order diagrams are taken into account. In addition to the aforementioned methods, E665 used an electromagnetic calorimeter to reject the electromagnetic background. Events are discarded if the fraction of energy deposited in the electromagnetic calorimeter to the energy transferred,  $\nu$ , exceeds some threshold value. The ratios, corrected for radiative background using either a numerical integration or the calorimeter have been found to be compatible within 5%. The  $x_{b,j}$  dependence of the cross-section ratio is shown in Fig.4. It decreases as  $x_{b,j}$  goes to 0, showing evidence of shadowing. On the other hand (Fig.5), no strong  $Q^2$  dependence is observed. Data points on Ca from NA28<sup>4</sup> are shown for comparison.

#### 3.3 Estimate of systematic errors

The sources and estimates of systematic uncertainty are as follow :

- *Beam normalization* : 0.7%
- *Target density* : 0.4%
- *Trigger acceptance* : due to difference in target size. Less than 3%.
- *Empty-target subtraction* : 1%
- *Time-dependent efficiency* : 4%
- *Radiative corrections* : 1.4%

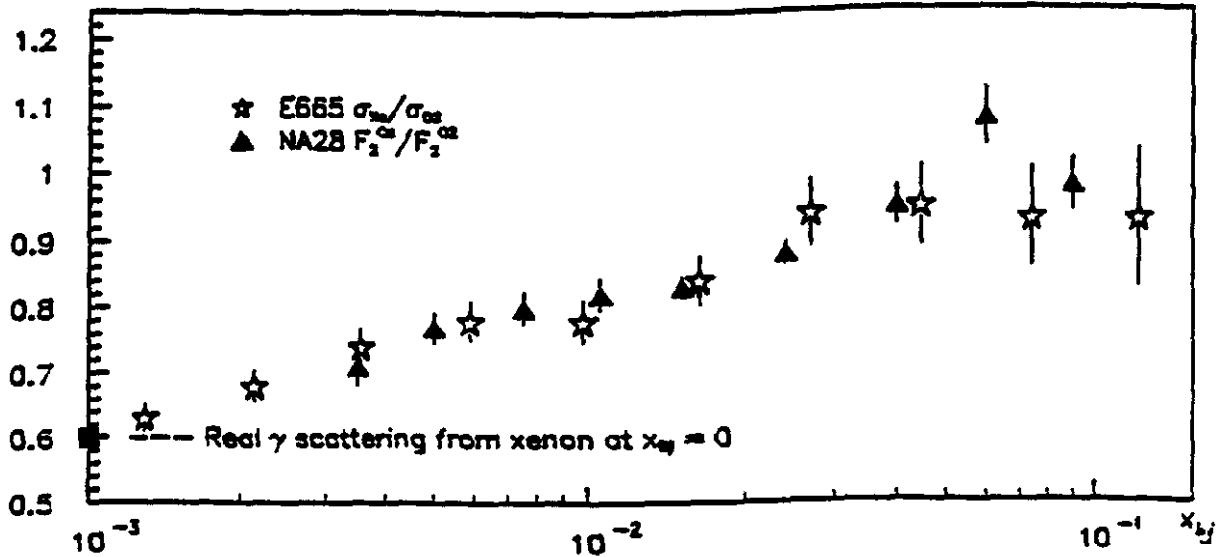


Fig. 4

Xe to D<sub>2</sub> cross-section ratio as a function of x<sub>b,j</sub>  
for Q<sup>2</sup> > 0.1 GeV<sup>2</sup>, ν > 40 GeV and y < 0.75

The Xe photo-production point has been obtained by interpolating the 60 GeV data from ref.5 on C, Cu and Pb and then extrapolating the value thus found from 60 GeV to 150 GeV using the energy dependence of the Cu data.

#### 4. Conclusion

The neutron-to-proton ratio has been measured by E665 in muon deep inelastic scattering at a beam energy of 490 GeV/c, for x<sub>b,j</sub> as low as 2 × 10<sup>-3</sup> and has been found to be consistent with 1 as x<sub>b,j</sub> goes to 0. The ratio of Xe to D<sub>2</sub> cross-sections has been measured for x<sub>b,j</sub> down to 10<sup>-3</sup> and shows evidence of shadowing, with no strong Q<sup>2</sup> dependence. Work is currently in progress to improve the understanding of systematic errors.

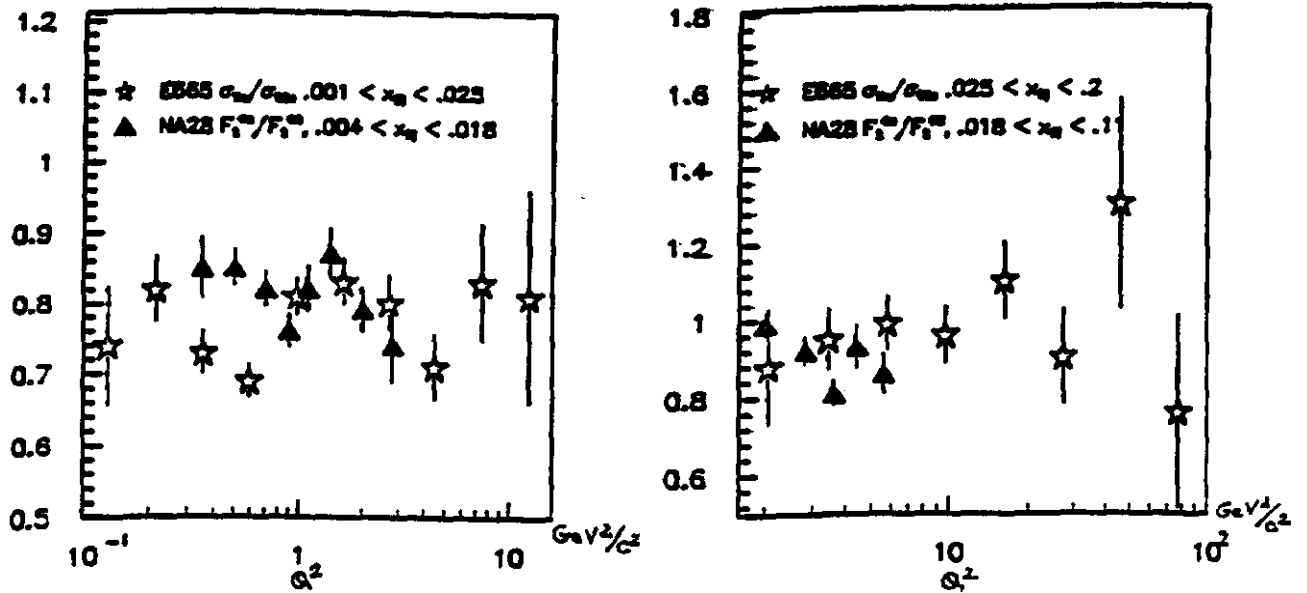


Fig. 5  
Xe to  $D_2$  cross-section ratio as a function of  $Q^2$

## 5. Acknowledgements

The work of the University of California, San Diego was supported in part by the National Science Foundation, contract numbers PHY82-05900, PHY85-11584 and PHY88-10221; the University of Illinois at Chicago by NSF contract PHY88-11164; and the University of Washington by NSF contract numbers PHY83-13347 and PHY86-13003. The University of Washington was also supported by the U. S. Department of Energy. The work of Argonne National Laboratory was supported by the Department of Energy, Nuclear Physics Division, under Contract No. W-31-109-ENGGG-38. The Department of Energy, High Energy Physics Division, supported the work of Harvard University, the University of Maryland, the Massachusetts Institute of Technology under Contract No. DE-AC02-76ER03069 and Yale University. The Albert-Ludwigs-Universität and the University of Wuppertal were supported in part by the Bundesministerium für Forschung und Technologie.

## 6. References

1. M.R. Adams et al., E665 Collaboration, to be published in *Nucl. Inst. and Meth.*
2. A.C. Benvenuti et al., BCDMS coll., *Phys. Lett. B237(1990) 601*

3. J.J. Aubert et al., EMC coll., *Nucl. Phys. B293(1987) 740*
4. A. Arneodo et al., *Nucl. Phys. B333(1990) 1*
5. D.O. Caldwell et al., *Phys. Rev. Lett. 42(1979) 553*